



Short communication

# An effective and stable Ni<sub>2</sub>P/TiO<sub>2</sub> catalyst for the hydrogenation of dimethyl oxalate to methyl glycolate

Hongmei Chen<sup>a</sup>, Jingjing Tan<sup>b,c</sup>, Yulei Zhu<sup>a,c,\*</sup>, Yongwang Li<sup>a,c</sup>

<sup>a</sup> Synfuels China Co. Ltd., Beijing 030006, PR China

<sup>b</sup> University of Chinese Academy of Sciences, Beijing 100049, PR China

<sup>c</sup> State Key Laboratory of Coal Conversion, Institute of Coal Chemistry, Chinese Academy of Sciences, Taiyuan 030001, PR China



## ARTICLE INFO

## Article history:

Received 7 August 2015

Received in revised form 2 October 2015

Accepted 5 October 2015

Available online 9 October 2015

## Keywords:

Dimethyl oxalate

Methyl glycolate

Hydrogenation

Ni<sub>2</sub>P

## ABSTRACT

An effective and stable bifunctional Ni<sub>2</sub>P/TiO<sub>2</sub> catalyst was proposed for gas-phase hydrogenation of dimethyl oxalate to corresponding alcohols. A 93.0% conversion of DMO with a selectivity of 88.0% to methyl glycolate was observed under 210 °C. Moreover, the catalyst showed an excellent stability which can be performed for 3600 h under the reaction conditions of 230 °C, 3 MPa H<sub>2</sub> and the weight space velocity of 0.1 h<sup>-1</sup>.

© 2015 Elsevier B.V. All rights reserved.

## 1. Introduction

Methyl glycolate (MG) is an important fine chemical intermediate, which can be used as a raw material for the synthesis of polyglycolic acid and other organic chemicals [1]. Ethylene glycol (EG) has benign properties and versatile functions, and it has been proposed as a raw material for producing many chemicals, including polyester, dynamite manufacture and antifreeze [2].

Several approaches envisioned for the production of MG have been reported [3,4]. Typically, severe reaction conditions were required to obtain a high yield of MG. For the production of EG, the primary route was the hydration of ethylene or fermentation of sugars [5–7]. However, these routes were limited for the shrinking oil and expensive bioprocesses. In contrast, the hydrogenation of dimethyl oxalate (DMO) to MG or EG is attractive as it is a more efficient and greener catalytic process (as seen in Scheme 1) [8].

EG can be achieved efficiently over copper-based catalysts via selective hydrogenation of DMO [9–11]. However, low MG yields (<83%) were obtained over copper-based catalysts [10,12], and the instability of the catalyst limited its further application. To improve the selectivity to MG in hydrogenation of DMO, introducing a noble metal to the catalytic system is required. For example, CuAu alloy nanoparticles and a silver-based catalyst were applied for the hydrogenation of DMO to obtain a high yield of MG (>90%) [13–15]. However, the large requirement of the noble metal limited its further application in industry. Thus, it is

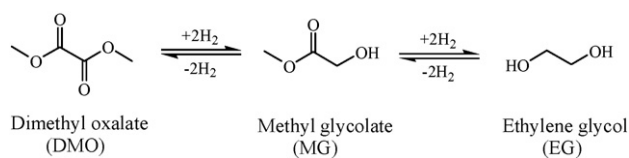
desirable but more challenging to design an efficient non-noble metal catalyst to catalyse the hydrogenation of DMO to MG under mild conditions. Because of their high catalytic efficiency and stability, the transition metal phosphides have been attracting increasing attention. Recently, many efforts demonstrated that the transition metal phosphide catalysts showed excellent activities for hydrodesulfurization, hydrodenitrogenation and hydrodeoxygenation owing to its strong noble metallic properties [16–20]. To the best of our knowledge, the transition metal phosphides have scarcely been reported in the hydrogenation of esters to their corresponding alcohols. Based on the above understandings, we hypothesise that it would be a huge breakthrough if the transition metal phosphides could replace the noble metal and be used for the DMO hydrogenation efficiently.

In this work, a bifunctional Ni<sub>2</sub>P/TiO<sub>2</sub> catalyst was proposed. The catalyst exhibited superior catalytic performance for the hydrogenation of DMO to MG. A high selectivity of 88.0% to MG with a 93.0% conversion of DMO was obtained under 210 °C. More importantly, the Ni<sub>2</sub>P/TiO<sub>2</sub> catalyst displayed an excellent stability, which can be successively performed for 3600 h without deactivation under 230 °C.

## 2. Experimental

The Ni<sub>2</sub>P/TiO<sub>2</sub> catalyst was prepared by temperature-programmed reducing method. The catalysts were characterized by ICP, XRD, TEM, XPS, BET, H<sub>2</sub>-TPR, and NH<sub>3</sub>-TPD. The catalytic performance evaluation was performed in a vertical fixed-bed reactor (i.d. 12 mm, length 600 mm) made of a stainless steel tube. Details of catalyst preparation,

\* Corresponding author at: Synfuels China Co. Ltd., Beijing 030006, PR China.  
E-mail address: zhuyulei@sxicc.ac.cn (Y. Zhu).



**Scheme 1.** The hydrogenation process of the DMO.

catalyst characterization, and catalyst evaluation are available in the supporting material.

### 3. Results and discussion

#### 3.1. Catalyst characterization

The textural properties derived from N<sub>2</sub> adsorption–desorption isotherms of the TiO<sub>2</sub> and Ni<sub>2</sub>P/TiO<sub>2</sub> catalysts are listed in Table 1. Compared with TiO<sub>2</sub> support, the BET surface area and average pore diameter of the Ni<sub>2</sub>P/TiO<sub>2</sub> catalyst decreased while the average pore volume enhanced. To understand the structures of the Ni<sub>2</sub>P/TiO<sub>2</sub> catalyst, XRD, TEM and XPS characterizations were performed. Fig. 1A shows the XRD patterns of the TiO<sub>2</sub> support and the as-prepared Ni<sub>2</sub>P/TiO<sub>2</sub> catalyst. For the Ni<sub>2</sub>P/TiO<sub>2</sub> catalyst, the three peaks positioned at 2θ = 40.8, 44.7, 47.5 are assigned to the (111), (021) and (210) lattice planes of Ni<sub>2</sub>P (JCPDS 65-9706), respectively. Fig. 1B shows the typical TEM (a) and HRTEM (c) images of the Ni<sub>2</sub>P/TiO<sub>2</sub> catalyst. The HRTEM analysis revealed that the crystal domains within Ni<sub>2</sub>P NPs had an interfringe distance of 0.22 nm, which is close to the lattice spacing of the (111) plane in face-centred cubic (fcc) Ni<sub>2</sub>P crystal (0.221 nm) [21,22]. Fig. 1C (a) displays the XPS spectra of the Ni<sub>2</sub>P/TiO<sub>2</sub> catalyst. The XPS spectrum for the fresh Ni<sub>2</sub>P/TiO<sub>2</sub> catalyst shows Ni (2p<sub>3/2</sub>) and P (2p<sub>3/2</sub>) peaks at 856.5 and 133.3 eV, respectively. The Ni (2p<sub>3/2</sub>) binding energy is consistent with the range of those reported for Ni (855.6–856.6 eV) in Ni(OH)<sub>2</sub> [23,24] while the P (2p<sub>3/2</sub>) binding energy is in good agreement with a value reported for P (133.3 eV) in Ni<sub>3</sub>(PO<sub>4</sub>)<sub>2</sub> [24,25]. As a result, the peaks at 856.5 and 133.3 eV are assigned to Ni<sup>2+</sup> and P<sup>5+</sup> species in the Ni<sub>2</sub>P, respectively. Meanwhile, additional peaks are observed in the Ni (2p<sub>3/2</sub>) and P (2p<sub>3/2</sub>) regions at 852.9–853.3 eV and 129.1–129.5 eV, respectively, which are assigned to reduced Ni<sup>δ+</sup> (0 < δ < 2) and P<sup>δ-</sup> (0 < δ < 1) in Ni<sub>2</sub>P [26,27]. The XPS for Ni metal and elemental phosphorus are reported to be at (852.5–852.9) and 130.2 eV, respectively [28]. A positive shift of 0.25–0.65 eV to 853.15 eV was observed for Ni (2p<sub>3/2</sub>) binding energies in the Ni<sub>2</sub>P catalyst (Fig. 1C), while a negative shift of 0.7 eV for the P (2p<sub>3/2</sub>) signal to 129.5 eV was obtained. These results verified that a few electrons were transferred from Ni to P. These results, combined with the X-ray powder diffraction (XRD) and TEM results further corroborated the formation of Ni<sub>2</sub>P NPs. In addition, the accessible surface acidic sites of the catalysts were probed by NH<sub>3</sub>-TPD (Fig. S1 in ESI†). Compared with TiO<sub>2</sub> and Ni/TiO<sub>2</sub>, the NH<sub>3</sub> desorption temperature of the Ni<sub>2</sub>P/TiO<sub>2</sub> catalyst shifted towards higher temperature. This result reflected that the addition of P increased the acidity and acid strength of the catalyst, as the formation of P–OH in the surface increased the Brønsted acid and the formation of electron-deficient state of Ni verified by XPS improved the Lewis acid [27].

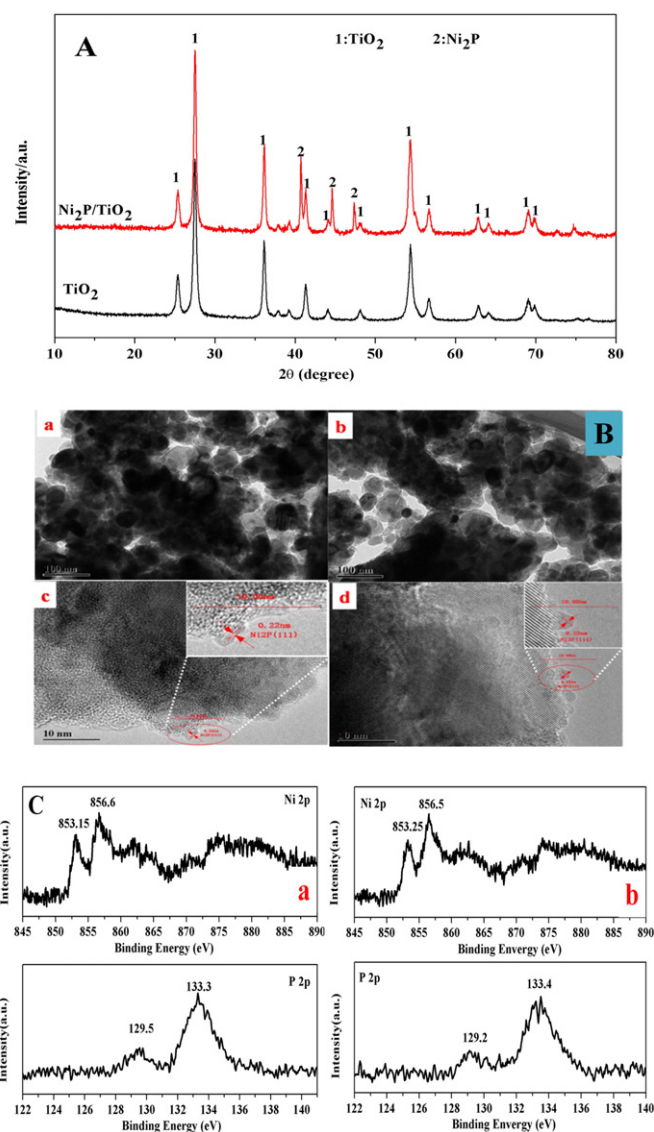


**Fig. 1.** (A) XRD patterns of as-prepared Ni<sub>2</sub>P/TiO<sub>2</sub> catalyst and TiO<sub>2</sub> support. (B) TEM and HRTEM images of the as-prepared (a and c) and spent (b and d) Ni<sub>2</sub>P/TiO<sub>2</sub> catalysts. (C) XPS spectra in the Ni (2p) and P (2p) regions for the as-prepared (a) and spent (b) Ni<sub>2</sub>P/TiO<sub>2</sub> catalysts.

#### 3.2. Catalytic test

Table 2 presents the results of the hydrogenation of DMO over TiO<sub>2</sub> (entries 1–2), Ni<sub>2</sub>P (entries 3–8), and Ni<sub>2</sub>P/TiO<sub>2</sub> (entries 9–15) catalysts. As shown in Table 2, the pure support of TiO<sub>2</sub> was inactive towards DMO hydrogenation, while a 38.2% conversion of DMO was observed with Ni<sub>2</sub>P as the catalyst at 200 °C (entry 3). Therefore, the Ni<sub>2</sub>P sites account for the catalytic hydrogenation performance. Additionally, it can be observed that the Ni<sub>2</sub>P catalyst exhibited a good selectivity of 90.5% to MG

**Table 1**

The physicochemical properties of TiO<sub>2</sub> and Ni<sub>2</sub>P/TiO<sub>2</sub> catalysts.

Catalyst	S <sub>BET</sub> (m <sup>2</sup> g <sup>-1</sup> )	D <sub>pore</sub> (nm)	V <sub>pore</sub> (cm <sup>3</sup> g <sup>-1</sup> )	Ni content <sup>a</sup> (mol/g)	P content <sup>a</sup> (mol/g)	Ni:P <sup>a</sup> (mole/mole)
TiO <sub>2</sub>	24.64	0.120	17.41	–	–	–
Ni <sub>2</sub> P/TiO <sub>2</sub> -fresh	15.43	0.097	22.65	1.62 × 10 <sup>-3</sup>	1.0 × 10 <sup>-3</sup>	1.62
Ni <sub>2</sub> P/TiO <sub>2</sub> -spent	16.35	0.106	22.02	1.33 × 10 <sup>-3</sup>	0.85 × 10 <sup>-3</sup>	1.56

<sup>a</sup> Determined by ICP.

# دانلود مقاله



<http://daneshyari.com/article/49398>



- ✓ امکان دانلود نسخه تمام متن مقالات انگلیسی
- ✓ امکان دانلود نسخه ترجمه شده مقالات
- ✓ پذیرش سفارش ترجمه تخصصی
- ✓ امکان جستجو در آرشیو جامعی از صدها موضوع و هزاران مقاله
- ✓ امکان پرداخت اینترنتی با کلیه کارت های عضو شتاب
- ✓ دانلود فوری مقاله پس از پرداخت آنلاین
- ✓ پشتیبانی کامل خرید با بهره مندی از سیستم هوشمند رهگیری سفارشات